

SYNTHESIS AND CHARACTERIZATION OF GALLIC ACID COMPLEXES WITH COBALT(II), NICKEL(II), AND COPPER(II) IONS: SPECTRAL ANALYSIS, X-RAY STRUCTURES, AND MICROSCOPIC IMAGING

Abdel Majid A. Adam^{1*}, Moamen S. Refat¹, Q. Mohsen¹ and Amnah Mohammed Alsuhaibani²

¹Department of Chemistry, College of Science, Taif University, P.O. Box 11099, Taif 21944, Saudi Arabia

²Department of Physical Sport Sciences, College of Sport Sciences & Physical Activity, Princess Nourah bint Abdulrahman University, P.O. Box 84428, Riyadh 11671, Saudi Arabia

(Received February 10, 2025; Revised March 13, 2025; Accepted March 13, 2025)

ABSTRACT. This study examines the synthesis, characterization, thermal stability, and microscopic analysis of gallic acid (abbreviated as GA) complexes formed with three transition metal ions: Co(II), Ni(II), and Cu(II). The researchers carried out a multi-step process, beginning with a series of chemical reactions between GA, acting as an organic ligand, and the respective metal ions. These reactions were conducted at a temperature of 65 °C and a pH of approximately 8, with a molar ratio of 2:1 between the GA ligand and the metal ion. The resulting products were referred to as the GA-Co complex, the GA-Ni complex, and the GA-Cu complex. Various physicochemical techniques were employed to thoroughly understand the structural, compositional, morphological, and thermal properties of the generated GA-Co, GA-Ni, and GA-Cu complexes, contributing to the field's knowledge. The synthesized complexes with Co(II), Ni(II), and Cu(II) ions have formulae of $(\text{NH}_4)_2[\text{Co}(\text{NH}_4\text{HL})_2(\text{H}_2\text{O})_2] \cdot 4\text{H}_2\text{O}$, $(\text{NH}_4)_2[\text{Ni}(\text{NH}_4\text{HL})_2(\text{H}_2\text{O})_2] \cdot 6\text{H}_2\text{O}$, and $(\text{NH}_4)_2[\text{Cu}(\text{NH}_4\text{HL})_2(\text{H}_2\text{O})_2] \cdot 5\text{H}_2\text{O}$, respectively. The complexation of the GA ligand with metal ions altered the microstructural features of the pristine ligand, as observed in the TEM images, indicating that the complexation significantly affected the microstructure of the synthesized materials.

KEY WORDS: Gallic acid, Metal ions, Spectroscopic techniques, Thermal decomposition, TEM

INTRODUCTION

Metal-based complexes are chemical compounds formed by the interaction between ligands and metals. These complexes are created by coordinating the central metal with the ligand using covalent bonds. This follows a donor-acceptor mechanism, where the ligand acts as the Lewis base, providing electron pairs, and the metal acts as the Lewis acid, accepting these electron pairs. Ligands can be organic or inorganic, anionic, cationic, or neutral, with one or more electron pairs to share with the metal [1-5]. Metal-based complexes have unique properties that enable diverse applications in science and industry [6, 7]. These complexes can interact with biological molecules, leading to medical applications. Researchers can optimize the effectiveness of metal complexes for therapeutic purposes, adjusting their properties to enhance anticancer activity and minimize side effects. Transition metals are used in the design and development of metal-based drugs, contributing to the treatment of various human conditions. Examples include platinum, vanadium, silver, gold, zinc, and lithium complexes used to treat cancer, diabetes, infections, diarrhea, and neurological diseases [8-17]. Other metal-based drugs include those containing iron, copper, and cobalt for treating anemia, Wilson's disease, and vitamin B deficiencies. Transition metal complexes have also shown utility in disease diagnosis. Metal-based compounds exhibit promises as anticancer agents due to their unique properties and ability to inhibit tumor growth [18, 19]. Platinum-based complexes are widely used and effective in cancer therapy, but face drawbacks like drug resistance, toxicity, and limited antitumor activity. This has motivated

*Corresponding authors. E-mail: majidadam@tu.edu.sa

This work is licensed under the Creative Commons Attribution 4.0 International License

research into non-platinum metal-based drugs as potentially more effective or less toxic alternatives, including those containing gold, ruthenium, palladium, and titanium. More recently, complexes with zinc, iron, copper, gold, and ruthenium have shown anticancer capabilities, with encouraging preclinical results. These metal-based compounds have the potential to revolutionize cancer treatment by providing new, more effective, and less toxic alternatives to platinum-based therapies, offering hope for improvement [20].

Gallic acid (Figure 1) is one of the simplest phenolic compounds found in plants. It is a naturally occurring polyphenol that is widely distributed throughout the plant kingdom. The IUPAC name of gallic acid is 3,4,5-trihydroxybenzoic acid [$C_6H_2(OH)_3COOH$]. This trihydroxybenzoic acid is classified as a phenolic acid, with its name derived from oak galls, which were historically used to produce tannic acid. Gallic acid has garnered considerable attention due to its ubiquity in various plants, such as vegetables, fruits, herbs, and medicinal species, including oak bark, tea leaves, pomegranates, gallnuts, berries, and grapes. In 1786, the renowned Swedish chemist Carl Wilhelm Scheele was the first to identify and isolate gallic acid and pyrogallic acid from plants. Since then, research on gallic acid and its derivatives has steadily increased, enhancing our understanding of this compound. Gallic acid possesses a range of potent biological and pharmacological activities, including antimicrobial, antioxidant, anti-inflammatory, and anti-tumor properties. These versatile characteristics have led to the widespread use of gallic acid in cosmetics, medicine, and as a food component [21, 22].

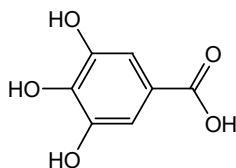


Figure 1. Molecular structure of gallic acid (3,4,5-trihydroxybenzoic acid).

In this study, we describe the synthesis, characterization, thermal stability, and microscopic analysis of gallic acid (abbreviated as GA) complexes formed with three transition metal ions: Co(II), Ni(II), and Cu(II). This objective was achieved through a multi-step process. Initially, we conducted a series of chemical reactions between GA, acting as an organic ligand, and the respective metal ions. These reactions were carried out at a temperature of 65 °C and a pH of approximately 8. The molar ratio between the GA ligand and the metal ion was 2:1. The products of the reactions between the GA ligand and the Co(II), Ni(II), and Cu(II) ions were designated as the GA-Co complex, the GA-Ni complex, and the GA-Cu complex, respectively. We then employed various physicochemical techniques to comprehensively understand the structural, compositional, morphological, and thermal properties of the generated GA-Co, GA-Ni, and GA-Cu complexes, providing a wealth of knowledge to the field. The synthesis and characterization of these GA complexes with transition metal ions are essential for understanding their potential applications in various fields, such as catalysis, sensors, and materials science.

EXPERIMENTAL

Chemicals

Sigma-Aldrich Chemical Company (St Louis, MO, USA) provided the metal chlorides used in this study, while Merck Chemical Company (KGaA, Germany) supplied the ligand and the methanol solvent. Both companies furnished the chemicals at analytical grade with the highest available purity. The chemicals utilized in the preparation included gallic acid (3,4,5-

3,4,5-trihydroxybenzoic acid; GA; 170.12 g/mol; purity \geq 98%), cobalt(II) chloride (CoCl_2 ; 129.84 g/mol; purity \geq 98%), nickel(II) chloride (NiCl_2 ; 129.60 g/mol; purity 98%), copper(II) chloride (CuCl_2 ; 134.45 g/mol; purity 99%), and HPLC-grade methanol. Appropriate safety precautions were implemented during the experiments, including the use of gloves, dust masks, and eye shields. These personal protective equipment measures were utilized throughout the study to safeguard the researchers and participants.

Synthesis

This study describes the synthesis, characterization, thermal stability, and microscopic analysis of the GA-Co, GA-Ni, and GA-Cu complexes. These complexes were prepared through a multi-step process. The initial step involves dissolving the reagents. The free GA ligand was dissolved in MeOH solvent (2 mmol in 25 mL), while the metal chlorides were dissolved in deionized water (2 mmol in 25 mL). Gentle heat was used to completely dissolve the reagents. The second step is the mixing of the reagents. Aqueous solutions (25 mL) of the Co(II), Ni(II), and Cu(II) ions were combined with 25 mL of methanolic GA ligand solution to obtain the GA-Co, GA-Ni, and GA-Cu mixed solutions. The third step is the optimization of the reaction conditions. The three beakers containing the GA-Co, GA-Ni, and GA-Cu mixed solutions were placed on a hot plate with a magnetic stirrer, and the stirring was initiated. The temperature of the reaction was optimized at 65 °C, and the pH was adjusted to approximately 8 using ammonia (5%). The reactions were carried out for 20 minutes of continuous stirring. The fourth step is collecting the products. The three beakers were left to evaporate until the solution volume was halved, and then they were left overnight to ensure complete precipitation. The final step is filtration and purification of the products. After standing overnight, white, dense precipitates were observed in each beaker; these precipitates were collected, filtered, and thoroughly washed with three systems: methanol, diethyl ether, and hot deionized water. The collected and purified GA-Co, GA-Ni, and GA-Cu complexes were oven-dried at 70 °C and stored in a desiccator containing anhydrous CaCl_2 . The synthesized complexes were subjected to various physicochemical techniques to comprehensively understand the structural, compositional, morphological, and thermal properties of the GA-Co, GA-Ni, and GA-Cu complexes.

Techniques for identification

FT-IR and UV-Vis spectra, obtained using a Thermo Scientific Nicolet iS10 FT-IR spectrometer and a Perkin-Elmer Lambda 25 UV/Vis spectrophotometer, respectively, were employed for comprehensive structural characterization of the GA-Mn, GA-Zn, and GA-Cd complexes. A Perkin-Elmer 2400 series II CHNS elemental analyzer was used to determine the carbon, nitrogen, and hydrogen content, which further verified the complexation stoichiometry between the investigated metal ions and the GA ligand. The XRD patterns and TEM images from a Philips X'Pert X-ray Diffractometer and a high-resolution JEM-2010 JEOL Transmission Electron Microscope, respectively, were used to observe the detailed microstructures of the synthesized GA-metal complexes. Finally, a Shimadzu TGA-50H thermal analyzer was utilized to thoroughly evaluate the thermal stability of the synthesized GA-metal complexes through comprehensive thermogravimetric (TG) and differential thermogravimetric (DTG) curves collected in the 25-800 °C range under an air atmosphere.

RESULTS AND DISCUSSION

Findings from conductivity and elemental analysis

The free GA ligand was dissolved in methanol solvent, while the Co(II), Ni(II), and Cu(II) chlorides were dissolved in water. The reaction between the GA ligand and the investigated metal

ions was carried out under specific conditions: i) the molar ratio was 2:1 (GA ligand to metal), ii) the solvent was a 1:1 methanol-water mixture, iii) the media was slightly basic (pH 8), and iv) the reaction temperature was 65 °C. Under these conditions, the GA ligand ($C_6H_2(OH)_3COOH$; H₄L) was deprotonated to form the $(NH_4HL)^-$ anion. The anion ligand was then coordinated the Co(II), Ni(II), and Cu(II) ions forming the following complexes:

(i) The GA-Co complex; $(NH_4)_2[Co(NH_4HL)_2(H_2O)_2].4H_2O$; a violet powder; chemical formula: $C_{14}H_{34}N_4O_{16}Co$ (573.37 g/mol). Elemental data analysis found (calculated): C, 29.10% (29.33); H, 6.15% (5.98); N, 9.62% (9.77); Co, 10.40% (10.28). (ii) The GA-Ni complex; $(NH_4)_2[Ni(NH_4HL)_2(H_2O)_2].6H_2O$; a light brown powder; chemical formula: $C_{14}H_{38}N_4O_{18}Ni$ (609.16 g/mol). Elemental data analysis found (calculated): C, 27.38% (27.60); H, 6.15% (6.29); N, 9.45% (9.20); Ni, 9.82% (9.64). (iii) The GA-Cu complex; $(NH_4)_2[Cu(NH_4HL)_2(H_2O)_2].5H_2O$; a brown powder; chemical formula: $C_{14}H_{36}N_4O_{17}Cu$ (596.0 g/mol). Elemental data analysis found (calculated): C, 28.40% (28.21); H, 6.22% (6.09); N, 9.58% (9.40); Cu, 10.40% (10.66).

The elemental analysis reveals that the synthesized complexes with Co(II), Ni(II), and Cu(II) ions possess formulae of $(NH_4)_2[Co(NH_4HL)_2(H_2O)_2].4H_2O$, $(NH_4)_2[Ni(NH_4HL)_2(H_2O)_2].6H_2O$, and $(NH_4)_2[Cu(NH_4HL)_2(H_2O)_2].5H_2O$, respectively. These formulas correspond to the overall compositions of $C_{14}H_{34}N_4O_{16}Co$, $C_{14}H_{38}N_4O_{18}Ni$, and $C_{14}H_{36}N_4O_{17}Cu$, respectively. The elemental data suggests a 1:2 metal-to-ligand ratio for all complexes. The conductance values provide information about the ionization state of metal-organic complexes. A HACH digital conductivity meter was used to measure the conductivity of the free GA ligand and its complexes at room temperature. The molar conductance of the free GA ligand in DMSO was $17.39 \Omega^{-1} \text{ cm}^2 \text{ mol}^{-1}$, indicating the ligand's non-conducting behavior. The molar conductance values of the GA-Co, GA-Ni, and GA-Cu complexes in DMSO were 79.06, 83.76, and $78.41 \Omega^{-1} \text{ cm}^2 \text{ mol}^{-1}$, respectively, suggesting the electrolytic nature of these complexes. The conductance data implies the presence of chloride ions either inside or outside the coordination sphere of the complexes. The presence of these chloride ions likely contributes to the electrolytic behavior observed in the GA metal complexes, in contrast to the non-conductive properties of the free GA ligand.

Findings from UV-Visible spectroscopic analysis

The solid GA free ligand and its complexes with the metal ions Co(II), Ni(II), and Cu(II) were dissolved in dimethylsulfoxide (DMSO) solution, and their solutions were analyzed using a UV-Visible spectrometer at a specific concentration (10⁻³ M). The generated UV-Visible spectra over the wavelength range from 200 to 1000 nm are shown in Figure 2. The UV-Visible spectrum of the uncomplexed GA ligand reveals that the free ligand absorbed over a wide range of wavelengths from 200 to 700 nm. Its UV-Visible profile is characterized by three absorption bands that appear in succession at 205, 330, and 442 nm. The band located at 205 nm is the weakest, the band at 330 nm is the strongest, and the band resonated at 442 nm is broad with medium-intensity. The width of the 442 nm band is approximately twice the width of the 330 nm band. The 205 nm band could be assigned to the $\pi \rightarrow \pi^*$ transitions, while the 330 and 442 nm bands could be attributed to the $n \rightarrow \pi^*$ transitions. Upon complexation with the metal ions, the band located at 205 nm in the UV-Visible spectrum of the GA free ligand was still observed in the spectra of its complexes with approximately the same intensity and position. Turning to the second band that characterized the UV-Visible spectrum of the GA at 330 nm, this band was observed in the same position with the same intensity in the GA-Co complex, and in the same position with half the intensity in the GA-Ni and GA-Cu complexes. The third absorption band that characterized the UV-Visible spectrum of the GA at 442 nm was no longer observed in the spectra of the GA-Co, GA-Ni, and GA-Cu complexes. The UV-Visible spectra of the GA-Co, GA-Ni, and GA-Cu complexes exhibited a new, very strong and very broad absorption band in the visible region located at 526, 530, and 520 nm, respectively. This band was not observed in the spectrum of the free GA ligand, and its presence in the spectra of the complexes confirms the

complexation process between the ligand and the investigated metal ions. The band that characterized the GA-Co complex at 526 nm had a width of approximately 250 nm, the band that characterized the GA-Ni complex at 530 nm had a width of approximately 225 nm, while the band that characterized the GA-Cu complex at 520 nm had a width of approximately 200 nm. The appearance of these characterized bands in the spectra of the metal complexes, along with the spectral changes in the characteristic absorption bands of the free GA ligand, can be attributed to the complexation process and potential GA ligand-to-metal charge transfer transitions. Furthermore, the UV-Visible profiles of the GA metal complexes suggest that the coordination of the Co(II), Ni(II), and Cu(II) metal ions to the GA ligand significantly impacts the electronic structure and optical properties of the free GA ligand.

Findings from FT-IR spectroscopic analysis

Figure 3 depicts the measured FT-IR spectra of the free GA ligand and the synthesized complexes. The main vibrational bands of the free GA ligand are assigned as follows:

Region 4000-1900 cm^{-1}

The spectral region between 4000 and 1900 cm^{-1} is characteristic of the $\nu(\text{C-H})$ vibrations of the aromatic ring, as well as the $\nu(\text{O-H})$ vibrations of the acidic and phenolic functional groups. In the IR spectrum of the free GA molecule, the observed band at 3491 cm^{-1} was attributed to the $\nu(\text{O-H})$ vibration of the phenolic group, while the band at 3269 cm^{-1} was assigned to the $\nu(\text{O-H})$ vibration of the acidic group. Additionally, the multiple bands observed at 3050 and 2990 cm^{-1} were characteristic of the asymmetric and symmetric C-H stretching vibrations.

Region 1800-1200 cm^{-1}

The spectral region between 1800 and 1200 cm^{-1} is characterized by the stretching vibrations resulted from the C-C, C=C, C-O, and C=O bonds. Additionally, this region exhibits OH deformations and ring deformations. In the IR spectrum of GA, the prominent bands observed at 1662, and 1537 cm^{-1} correspond to the $\nu(\text{C=O})$ stretching vibrations of the carboxylic group and the $\nu(\text{C=C})$ vibrations of the aromatic ring, respectively. The bands at 1260, 1382, and 1606 cm^{-1} are attributed to the $\nu(\text{C-O})$, in-plane $\delta(\text{O-H})$, and in-plane $\delta_{\text{def}}(\text{C-H})$ vibrations, respectively.

Region 1200-1000 cm^{-1}

In the spectral region between 1200 and 1000 cm^{-1} , multiple modes exhibit strong coupling, including ring torsion, ring deformation, $\nu(\text{C-C})$, and in-plane and out-of-plane C-H deformations. The IR spectrum of GA shows bands at 1021 and 1212 cm^{-1} corresponding to the $\nu(\text{C-C})$ and $\nu(\text{C-O})$ vibrations, respectively.

Region below 1000 cm^{-1}

The free GA ligand exhibited three distinctive bands in this spectral region. These bands were observed at 764, 862, and 898 cm^{-1} , corresponding to ring stretching vibrations, out-of-plane $\delta(\text{O-H})$, and out-of-plane $\delta(\text{C-H})$ vibrations, respectively.

A comprehensive analysis of the relevant IR spectral bands of the unbound GA ligand and the corresponding bands in the IR spectra of its complexes with Co(II), Ni(II), and Cu(II) ions reveals a variety of characteristic bands of the GA molecule that exhibit noticeable shifts in frequency

and significant changes in their band intensities upon metal ion coordination. The observed changes in position and intensity of certain IR bands of the GA ligand indicate that the GA molecule undergoes substantial structural and electronic modifications when it coordinates to the metal centers in the respective complexes, highlighting the complexity of our research. The GA molecule has two characteristic functional groups: a carboxylic group (COOH) and three hydroxyl groups (OH). The vibrational mode of the phenolic group produces a sharp and intense absorption IR band at 3491 cm^{-1} , while the vibrational mode of the acidic group creates a broad and intense IR band with a conical shape at 3269 cm^{-1} . Following the complexation of GA with the investigated metal ions, the characteristic bands of the $\nu(\text{O-H})$ vibrational modes were no longer observed in the IR spectra of the complexes, indicating deprotonation. This suggests that the GA molecule undergoes deprotonation upon complexation with the metal ions, leading to the disappearance of the characteristic IR bands associated with the $\nu(\text{O-H})$ vibrational modes of the functional groups. The deprotonated O-H groups of GA molecule involved in the complexation with the investigated metal ions, and this has resulted in the formation of new and weak IR bands at 534 , 546 , and 541 cm^{-1} for the GA-Co, GA-Ni, and GA-Cu complex, respectively, arising from the $\nu(\text{M-O})$ vibrational modes [23]. The metal complex containing the Co(II) ion displayed several absorption bands at 1630 , 829 , 716 , and 628 cm^{-1} corresponding to the $\delta_{\text{b}}(\text{H}_2\text{O})$, $\delta_{\text{rock}}(\text{H}_2\text{O})$, $\delta_{\text{wag}}(\text{H}_2\text{O})$, and $\delta_{\text{twist}}(\text{H}_2\text{O})$ vibrational modes of the coordinated water molecules, respectively. Similarly, the complex containing the Ni(II) ion exhibited corresponding wavenumbers of 1632 , 830 , 710 , and 633 cm^{-1} . For the GA-Cu complex, these absorption bands were observed at 1629 , 828 , 712 , and 627 cm^{-1} , respectively [24]. Based on stoichiometry and spectroscopy results, a proposed chemical structure for the GA metal-based complexes is presented in Figure 4.

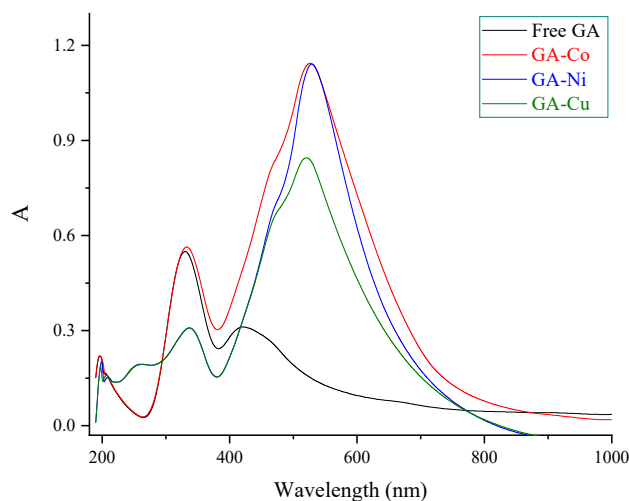


Figure 2. The UV-Visible absorption spectra of the uncomplexed GA ligand and its coordination complexes with Co(II), Ni(II), and Cu(II) ions.

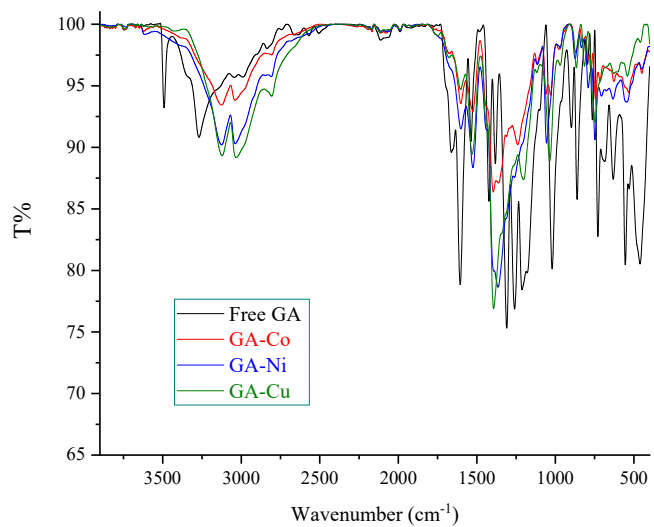
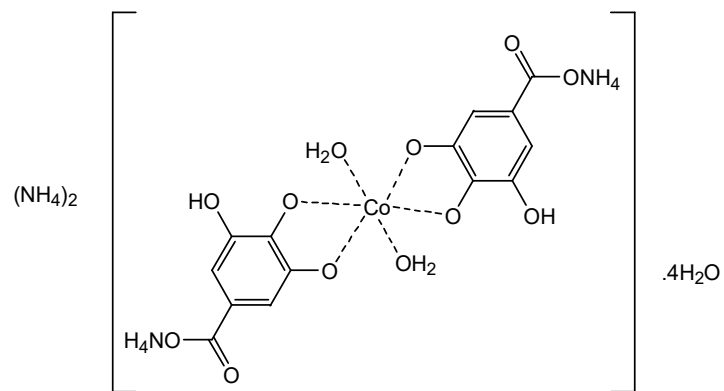


Figure 3. The FT-IR spectra of the uncomplexed GA ligand and its coordination complexes with Co(II), Ni(II), and Cu(II) ions.



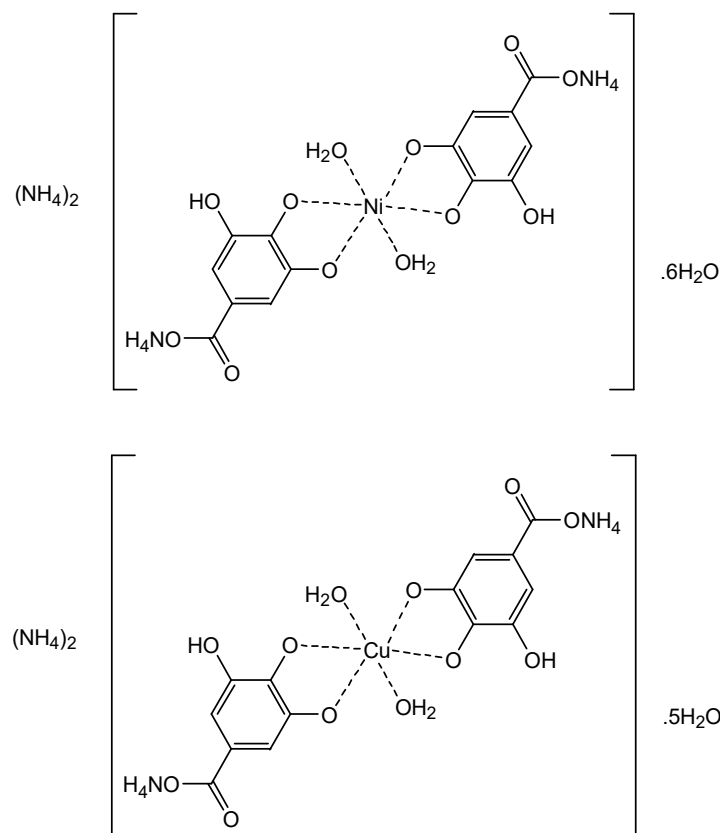


Figure 4. The suggested chemical structures of the GA-Co, GA-Ni, and GA-Cu complexes.

XRD and TEM observations

XRD and TEM techniques were employed to characterize the X-ray structures, phase purity, and particle shapes of the synthesized GA-Co, GA-Ni, and GA-Cu complexes. These complexes, as well as the free GA ligand, were analyzed using an X-ray diffraction technique equipped with a Cu K_{α1} X-ray source and a Ge monochromator. The XRD measurements were conducted at an operating voltage of 40 kV, a current of 30 mA, and a temperature of 25 °C. The XRD spectral data collected within the angular range of 5 to 70° for the compounds is presented in Table 1. The XRD patterns of the unbound GA ligand revealed four distinctive peaks at 2θ values of 16.353°, 19.300°, 25.502°, and 43.054°. The peak at 19.300° was the most intense and prominent, while the other three exhibited moderate intensities. Additionally, the GA ligand showed four more low-intensity peaks. The XRD profile of the GA-Co complex showed two distinctive peaks. A prominent and intense peak was detected at a Bragg's angle 2θ of 32.959°, while a moderately intense peak was observed at a 2θ value of 58.584°. The XRD diffractogram of the GA-Ni complex exhibits three characteristic XRD reflections: a very strong intensity line at 2θ 11.542°, a medium-intensity diffraction at 2θ 32.651°, and a low-intensity diffraction at 2θ 58.30°. The complex containing the Cu(II) ion displayed two prominent XRD diffraction peaks, one at 32.679°

which was very strong and intense, and another at 58.352° which was of medium intensity. Generally, the XRD patterns of the GA-Co complex, GA-Ni complex, and GA-Cu complex indicated that these complexes possessed well-organized and well-defined structures. The well-defined and organized structures of these complexes, as shown by their XRD patterns, suggest that they have a high degree of crystallinity and a consistent arrangement of atoms or molecules within their respective frameworks. The inter-planar spacing between the atoms (termed as *d*-spacing) for the highest-intensity peaks of the GA-Co, GA-Ni, and GA-Cu complexes were 2.71549 Å, 2.74039 Å, and 2.73808 Å, respectively. The corresponding full width at half-maximum (termed as FWHM) values for these peaks were 0.332° , 0.361° , and 0.352° , respectively.

A high-resolution transmission electron microscope (TEM) was employed to capture the TEM images, which were then used to observe the morphology, distribution, and particle sizes of the complexes. The TEM images provide detailed information about the structural characteristics and distribution of the complexes, allowing for a comprehensive understanding of their properties and potential applications. Figure 5 presents the TEM images of the uncomplexed GA ligand, as well as the synthesized GA-Co, GA-Ni, and GA-Cu complexes. The uncomplexed GA ligand particles tend to be individual and not aggregated, exhibiting a closed-ended, water lily-like rhizome shape. In general, the ligand particles display a similar shape and size, with diameters ranging from 100 to 120 nm. The interesting water lily-like rhizome shape of the ligand particles was altered when it was complexed with the investigated metal ions to form the GA-Co, GA-Ni, and GA-Cu complexes. The TEM images of these complexes indicated that their particles have a stone-like appearance, suggesting a change in the morphology and aggregation behavior of the ligand upon complexation with the metal ions. These stone-like particles exhibit varying sizes and tend to aggregate into cluster-like formations, potentially indicating the formation of larger, higher-order structures. Most particles of these complexes had diameters within the range of 75-150 nm, indicating a range of particle sizes in the resulting metal-ligand complexes.

Table 1. The XRD spectral data of the strongest lines for the uncomplexed GA ligand and its coordination complexes with Co(II), Ni(II), and Cu(II) ions.

Compound	2θ (deg)	<i>d</i> -spacing value; (Å)	FWHM (deg)	Gross intensity
Free GA	16.353	5.41613	0.292	1211
	19.300	4.59517	0.290	784
	25.502	3.49001	0.319	627
	43.054	2.09925	0.249	354
GA-Co	32.959	2.71549	0.332	509
	58.584	1.57441	0.449	362
GA-Ni	11.542	7.66041	0.335	1037
	32.651	2.74039	0.361	565
	58.304	1.58131	0.417	284
GA-Cu	32.679	2.73808	0.352	609
	58.352	1.58013	0.410	265

Thermal observations

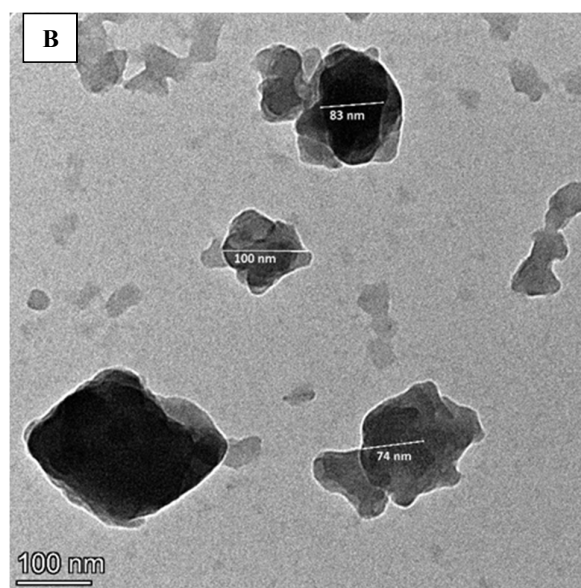
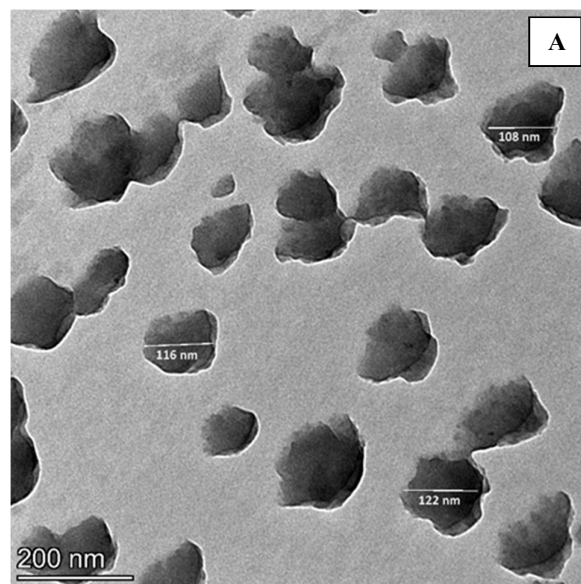
The compositions of the synthesized complexes containing Co(II), Ni(II), and Cu(II) ions were $(\text{NH}_4)_2[\text{Co}(\text{NH}_4\text{HL})_2(\text{H}_2\text{O})_2] \cdot 4\text{H}_2\text{O}$, $(\text{NH}_4)_2[\text{Ni}(\text{NH}_4\text{HL})_2(\text{H}_2\text{O})_2] \cdot 6\text{H}_2\text{O}$, and $(\text{NH}_4)_2[\text{Cu}(\text{NH}_4\text{HL})_2(\text{H}_2\text{O})_2] \cdot 5\text{H}_2\text{O}$, respectively. These compositions were proposed based on spectral, elemental, and conductivity data. The next step to verify the proposed compositions and structures of these complexes is to characterize them through thermal analysis. Thermal analysis can provide insight into the thermal stability and confirm the structural characteristics. Table 2

lists the potential thermal degradation patterns for the uncomplexed GA ligand and its coordination complexes with Co(II), Ni(II), and Cu(II) ions. The observed weight losses were consistent with the expected weight losses at each decomposition step for the free GA ligand, the GA-Co complex, the GA-Ni complex, and the GA-Cu complex. While the uncomplexed GA ligand exhibited excellent thermal stability, able to withstand temperatures up to 225 °C, complexing the ligand with Co(II), Ni(II), and Cu(II) ions significantly decreased its thermal stability, reducing it to below 150 °C. Specifically, the GA-Co, GA-Ni, and GA-Cu complexes began to thermally degrade at approximately 120 °C, with GA-Co > GA-Cu, which was attributed to the strength of the metal-ligand coordination. The complex containing the Cu(II) ion went through a three-step degradation process, while the complexes with Co(II) and Ni(II) ions experienced a two-step degradation process. The thermal decomposition of the GA-Co, GA-Ni, and GA-Cu complexes resulted in the final production of CoO, NiO, and CuO oxides, respectively. These metal oxide compounds contain no residual carbon from the decomposition process. The calculated and experimental percentages of the expelled moieties from the GA-metal based complexes are closely aligned, which strongly corroborates the stoichiometry determined through experimentation.

The uncomplexed GA ligand exhibits thermal stability up to 225 °C, as shown by its thermogram. The ligand's decomposition commenced at 225 °C and concluded at 600 °C. It underwent a single degradation step, characterized by a DTG_{max} of 284 °C, resulting in a corresponding weight loss of (calculated; 100.0%, observed; 99.75%). The thermoanalytical investigation of the GA-Co and GA-Ni complexes revealed a two-step decomposition process. The GA-Co complex underwent decomposition at maximum DTG temperatures of 236 °C and 552 °C, resulting in weight losses of 30.25% (calculated; 30.70%) and 55.72% (calculated; 56.16%), respectively. Similarly, the GA-Ni complex decomposed at maximum DTG temperatures of 270 °C and 416 °C, with weight losses of 34.27% (calculated; 34.80%) and 52.49% (calculated; 52.86%), respectively. The final decomposition stage for both complexes culminated in the formation of CoO and NiO as the ultimate products, without any leftover carbon. The GA-Cu complex experienced thermal decomposition in roughly three phases within the temperature range of 110-800 °C. The first mass loss (observed; 15.30%, calculated; 15.10%), with a peak at DTG_{max} of 130 °C, was attributed to the release of five water molecules. In the second phase from 150-320 °C (observed; 17.50%, calculated; 17.45%), the maximum decomposition rate at 281 °C was reasonably attributed to the loss of two water and four ammonia molecules. The third decomposition step, with a maximum around 355 °C and occurring within the 320-800 °C range, was likely due to the removal of the organic compound C₁₄H₁₀O₉. This final stage of degradation leaves behind CuO as the end product, with no carbon remaining.

Table 2. The thermal decomposition results of the uncomplexed GA ligand and the synthesized GA-Co, GA-Ni, and GA-Cu complexes.

Compound	Stages	TG range (°C)	DTG max. (°C)	TG% mass loss		Lost species
				Found	Calculated	
Free GA	I	225-600	284	99.75	100.0	2C ₂ H ₂ + 3CO ₂ + H ₂
GA-Co complex	I	120-260	236	30.25	30.70	6H ₂ O + 4NH ₃
	II	260-800	552	55.72	56.16	C ₁₄ H ₁₀ O ₉
	Residue	-	-	13.40	13.07	CoO
GA- Ni complex	I	130-325	270	34.27	34.80	8H ₂ O + 4NH ₃
	II	270-800	416	52.49	52.86	C ₁₄ H ₁₀ O ₉
	Residue	-	-	12.50	12.26	NiO
GA- Cu complex	I	110-150	130	15.30	15.10	5H ₂ O
	II	150-320	281	17.50	17.45	2H ₂ O + 4NH ₃
	III	320-800	355	53.48	54.03	C ₁₄ H ₁₀ O ₉
	Residue	-	-	13.09	13.35	CuO



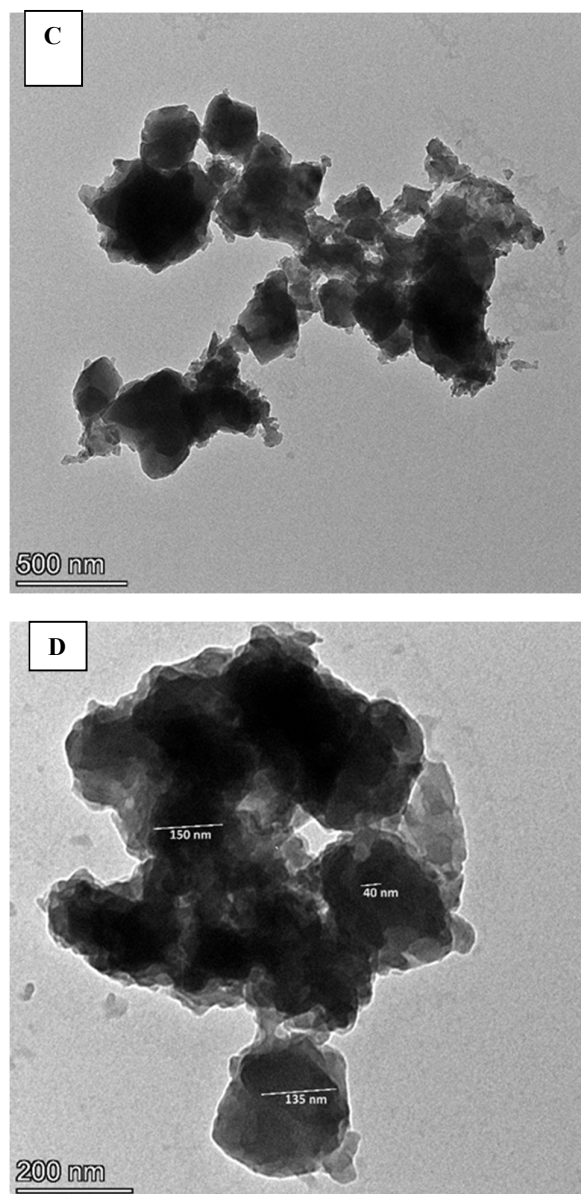


Figure 5. The TEM images of A) the free GA ligand, B) the GA-Co complex, C) the GA-Ni complex, and D) the GA-Cu complex.

CONCLUSION

This study investigates the synthesis, characterization, thermal stability, and microscopic analysis of gallic acid (GA) complexes formed with three transition metal ions: Co(II), Ni(II), and Cu(II). The researchers carried out a multi-step process, beginning with a series of chemical reactions between GA, acting as an organic ligand, and the respective metal ions. These reactions were performed at a temperature of 65 °C and a pH of approximately 8, with a molar ratio of 2:1 between the GA ligand and the metal ion. The resulting products were referred to as the GA-Co complex, the GA-Ni complex, and the GA-Cu complex. Various physicochemical techniques were used to thoroughly understand the structural, compositional, morphological, and thermal properties of the generated GA-Co, GA-Ni, and GA-Cu complexes. The synthesized complexes with Co(II), Ni(II), and Cu(II) ions have formulae of $(\text{NH}_4)_2[\text{Co}(\text{NH}_4\text{HL})_2(\text{H}_2\text{O})_2] \cdot 4\text{H}_2\text{O}$, $(\text{NH}_4)_2[\text{Ni}(\text{NH}_4\text{HL})_2(\text{H}_2\text{O})_2] \cdot 6\text{H}_2\text{O}$, and $(\text{NH}_4)_2[\text{Cu}(\text{NH}_4\text{HL})_2(\text{H}_2\text{O})_2] \cdot 5\text{H}_2\text{O}$, respectively. The complexation of the GA ligand with metal ions altered the microstructural features of the pristine ligand, as observed in the TEM images, indicating that the complexation significantly affected the microstructure of the synthesized materials. The findings of this study provide valuable insights into the formation, characterization, and properties of these GA-metal complexes, which can have potential applications in various fields, such as catalysis, sensors, and biomedical applications.

ACKNOWLEDGEMENT

The authors extend their appreciation to Taif University, Saudi Arabia, for supporting this work through project number (TU-DSPP-2024-78).

Funding

This research was funded by Taif University, Saudi Arabia, Project No. (TU-DSPP-2024-78).

REFERENCES

1. Almehezia, A.A.; Alkahtani, H.M.; Zen, A.A.; Obaidullah, A.J.; Naglah, A.M.; Alzughaibi, M.M.; Eldaroti, H.H. Complexes of the antibiotic drug succinylsulfathiazole with the La(III), Sm(III), and Tb(III) ions: Spectral characterizations, microscopic pictures, and thermal properties. *Bull. Chem. Soc. Ethiop.* **2025**, *39*, 327-339.
2. Alsawat, M.; Adam, A.M.A.; Refat, M.S.; Alsuhaibani, A.M.; El-Sayed, M.Y. Structural, spectroscopic, and morphological characterizations of metal-based complexes derived from the reaction of 1-phenyl-2-thiourea with Sr^{2+} , Ba^{2+} , Cr^{3+} , and Fe^{3+} ions. *Bull. Chem. Soc. Ethiop.* **2024**, *38*, 1803-1814.
3. Adam, A.M.A.; Refat, M.S.; Alsuhaibani, A.M.; El-Sayed, M.Y. Preparation and characterizations of metal-based complexes derived from the reaction of Trizma base with Mg(II), Ca(II), and Ba(II) ions. *Bull. Chem. Soc. Ethiop.* **2024**, *38*, 1791-1801.
4. El-Habeeb, A.A.; Refat, M.S. Synthesis, spectroscopic characterizations and biological studies on gold(III), ruthenium(III) and iridium(III) complexes of trimethoprim antibiotic drug. *Bull. Chem. Soc. Ethiop.* **2024**, *38*, 701-714.
5. Alsuhaibani, A.M.; Adam, A.M.A.; Refat, M.S.; Kobeasy, M.I.; Bakare, S.B.; Bushara, E.S. Spectroscopic, thermal, and anticancer investigations of new cobalt(II) and nickel(II) triazine complexes. *Bull. Chem. Soc. Ethiop.* **2023**, *37*, 1151-1162.
6. Eichhorn, G.L.; Marzilli, L.G. *Advances in Inorganic Biochemistry Models in Inorganic Chemistry*, PTR Prentice-Hall, Inc, New Jersey; **1994**.
7. Hughes, M.N. *The Inorganic Chemistry of Biological Processes*, 2nd ed., Wiley: Chichester [England]; **1984**.

8. Younes, A.A.O.; Refat, M.S.; Saad, H.A.; Adam, A.M.A.; Alzoghbi, O.M.; Alsulaim, G.M.; Alsuhaibani, A.M. Complexation of some alkaline earth metals with bidentate uracil ligand: Synthesis, spectroscopic and antimicrobial analysis. *Bull. Chem. Soc. Ethiop.* **2023**, *37*, 945-957.
9. Alkathiri, A.A.; Atta, A.A.; Refat, M.S.; Altalhi, T.A.; Shakya, S.; Alsawat, M.; Adam, A.M.A.; Mersal, G.A.M.; Hassanien, A.M. Preparation, spectroscopic, cyclic voltammetry and DFT/TD-DFT studies on fluorescein charge transfer complex for photonic applications. *Bull. Chem. Soc. Ethiop.* **2023**, *37*, 515-532.
10. Adam, A.M.A.; Refat, M.S.; Gaber, A.; Grabchev, I. Complexation of alkaline earth metals Mg^{2+} , Ca^{2+} , Sr^{2+} and Ba^{2+} with adrenaline hormone: Synthesis, spectroscopic and antimicrobial analysis. *Bull. Chem. Soc. Ethiop.* **2023**, *37*, 357-372.
11. Al-Hazmi, G.H.; Adam, A.M.A.; El-Desouky, M.G.; El-Bindary, A.A.; Alsuhaibani, A.M.; Refat, M.S. Efficient adsorption of Rhodamine B using a composite of $Fe_3O_4@zif-8$: Synthesis, characterization, modeling analysis, statistical physics and mechanism of interaction. *Bull. Chem. Soc. Ethiop.* **2023**, *37*, 211-229.
12. Alsuhaibani, A.M.; Adam, A.M.A.; Refat, M.S. Four new tin(II), uranyl(II), vanadyl(II), and zirconyl(II) alloxan biomolecule complexes: Synthesis, spectroscopic and thermal characterizations. *Bull. Chem. Soc. Ethiop.* **2022**, *36*, 373-385.
13. Al-Hazmi, G.H.; Alibrahim, K.A.; Refat, M.S.; Ibrahim, O.B.; Adam, A.M.A.; Shakya, S. A new simple route for synthesis of cadmium(II), zinc(II), cobalt(II), and manganese(II) carbonates using urea as a cheap precursor and theoretical investigation. *Bull. Chem. Soc. Ethiop.* **2022**, *36*, 363-372.
14. Alsuhaibani, A.M.; Refat, M.S.; Adam, A.M.A.; Kobeasy, M.I.; Kumar, D.N.; Shakya, S. Synthesis, spectroscopic characterizations and DFT studies on the metal complexes of azathioprine immunosuppressive drug. *Bull. Chem. Soc. Ethiop.* **2022**, *36*, 73-84.
15. El-Sayed, M.Y.; Refat, M.S.; Altalhi, T.; Eldaroti, H.H.; Alam, K. Preparation, spectroscopic, thermal and molecular docking studies of covid-19 protease on the manganese(II), iron(III), chromium(III) and cobalt(II) creatinine complexes. *Bull. Chem. Soc. Ethiop.* **2021**, *35*, 399-412.
16. Alosaimi, A.M.; Saad, H.A.; Al-Hazmi, G.H.; Refat, M.S. In situ acetonitrile/water mixed solvents: An ecofriendly synthesis and structure Explanations of Cu(II), Co(II), and Ni(II) complexes of thioxoimidazolidine. *Bull. Chem. Soc. Ethiop.* **2021**, *35*, 351-364.
17. Refat, M.S.; Altalhi, T.A.; Al-Hazmi, G.H.; Al-Humaidi, J.Y. Synthesis, characterization, thermal analysis and biological study of new thiophene derivative containing o-aminobenzoic acid ligand and its Mn(II), Cu(II) and Co(II) metal complexes. *Bull. Chem. Soc. Ethiop.* **2021**, *35*, 129-140.
18. Mojos, K.D.; Orvig, C. Metallodrugs in medicinal inorganic chemistry. *Chem. Rev.* **2014**, *114*, 4540-4563.
19. Alessio, E. *Bioinorganic Medicinal Chemistry*, Wiley-VCH Verlag GmbH and Co. KGaA: Germany; **2011**.
20. Ott, I.; Gust, R. Non platinum metal complexes as anti-cancer drugs. *Arch. Pharm.* **2007**, *340*, 117-126.
21. Fernandes, F.H.A.; Salgado, H.R.N. Gallic acid: Review of the methods of determination and quantification. *Crit. Rev. Anal. Chem.* **2016**, *46*, 257-265.
22. Badhani, B.; Sharma, N.; Kakkar, R. Gallic acid: A versatile antioxidant with promising therapeutic and industrial applications. *RSC Adv.* **2015**, *5*, 27540-27557.
23. Bellamy, L.J. *The infrared Spectra of Complex Molecules*, Chapman & Hall: London; **1975**.
24. Deacon, G.B.; Phillips, R.J. Relationships between the carbon-oxygen stretching frequencies of carboxylato complexes and the type of carboxylate coordination. *Coord. Chem. Rev.* **1980**, *33*, 227-250.